Available online at www.sciencedirect.com
SCIENCE DIRECT®
Journal of Power Sources 119–121 (2003) 538–542
JOURNAL OF POWER SOURCES
www.elsevier.com/locate/jpowsour

Electrochemical behavior of graphite anode at elevated temperatures in organic carbonate solutions

M.D. Levi*, C. Wang, J.S. Gnanaraj, D. Aurbach

Department of Chemistry, Bar-Ilan University, Ramat-Gan 52900, Israel

Abstract

A combination of three major electroanalytical techniques (slow-scan rate cyclic voltammetry (SSCV), potentiostatic intermittent titration (PITT) and electrochemical impedance spectroscopy (EIS)) was applied for comprehensive analysis of temperature dependence of the most important equilibrium and kinetic parameters related to the Li-insertion process. These parameters include the differential intercalation capacity, C_{int} and the chemical diffusion coefficient, D_{chem}. We have analyzed the complicated, ambivalent influence of the temperature on the shape of the cyclic voltammety curves, probing the rate of separate steps of the intercalation process close to equilibrium. Good agreement had been found between the SSCV data measured over a wide range of temperatures, and the classical staging phase diagram of Li_xC_6 (this diagram is presented as a plot of the absolute temperature, T versus intercalation level, x).

Keywords: Lithium rechargeable batteries; Lithiated graphite electrodes; The chemical diffusion coefficient of Li-ion; Elevated temperatures; Staging phase diagram

1. Introduction

It is well known that button-type cells may provide much better long-term cyclability and rate capability of intercalation electrodes compared to the same characteristics obtained with the use of large, flooded cells. The mass of the electrodes can be chosen as the same, whereas the mass of the solution in contact with the electrode in the button cell may be an order of magnitude less compared to that in the flooded cell. The dependence of the electrochemical behavior of intercalation electrodes on the WE to the solution mass ratio can be explained by the inevitable presence of some reducible species, even in trace concentrations, in the solution, which affects detrimentally the electrode's cycling and rate capability. Our preliminary electroanalytical characterizations of Li-intercalation into graphite showed that this effect was especially pronounced when the electrode was cycled at elevated temperatures. Notice that a similar problem related to the WE to electrolyte mass ratio may appear when a long-term characterization of intercalation electrodes is required, i.e. by using electrochemical impedance spectroscopy (EIS) down to very low frequency. Recently, an original three-electrode button cell design was described for such long-term EIS characterizations of composite graphite electrode at room temperature [1]. Here, we applied a slightly modified three-electrode button cell design compared to that presented in [1]. Then a special cell test protocol was developed, involving the combination of three basic electroanalytical techniques: slow-scan rate cyclic voltammetry (SSCV), potentiostatic intermittent titration (PITT) and EIS. When used properly, the combination of these three techniques covers almost completely the spectrum of individual relaxation processes contributing to the overall process of battery charging, discharging and rest. During recent years, we have advanced and optimized such an approach for the study of the electrochemistry of intercalation electrodes using experimental flooded electrochemical cells operating at room temperature [2–4]. Here, this approach was adapted for fine electroanalytical characterizations of graphite anodes at elevated temperatures in organic carbonate-based solutions. Because of the limited size of this presentation we restricted our discussion of the experimental results obtained to the temperature dependence of SSCV and PITT responses only. Temperature dependence of the related EIS characteristics will be reported elsewhere [5].

2. Experimental

The preparation of thin composite graphite electrodes with a typical mass of several milligrams had been described

* Corresponding author.
E-mail address: levimi@mail.biu.ac.il (M.D. Levi).

0378-7753/03/$ – see front matter
doi:10.1016/S0378-7753(03)00279-9

previously [2]. Here, we used commercial graphite powder KS-15 (Lonza), 90%, and a PVDF binder, 10%. The average mass of the electrode was 2 ± 0.1 mg. The preparation of three-electrodes button cells based on standard 2032 coin-type cells (NRC, Canada), containing a composite graphite disc working electrode, and lithium foil counter and reference electrodes was very similar to that described by Martinent et al. [1]. The only difference was that we inserted an additional glassy paper layer between the WE and the Cellgard polypropylene membrane. A thin strip of Li-reference electrode was pressed on a Ni wire. The upper part of the wire was carefully isolated from both electrodes and the stainless steel framework was isolated by a thin Teflon tape. The cell was hermetically closed in a standard crimping device. The NRC (Canada) cells were additionally isolated with an epoxy glue. These cells allowed us to reversibly cycle the graphite electrodes at elevated temperatures several hundred times without any deterioration of their reversible capacity. The cells were thermostated at different temperatures with an accuracy of ± 0.5 °C.

The electrolyte solution was 1 M $LiPF_6$ (Merck) in an ethylene carbonate (EC) + dimethylcarbonate (DMC) 1:1 mixture (Li-battery grade from Merck, KGaA) in the presence of different concentrations of dimethyl pyrocarbonate (DMPC). The latter additive was found to be a very good stabilizer for graphite electrodes.

SSCV and PITT techniques were applied using a computerized potentiostat–galvanostat Model 20 Autolab controlled by the GPES Version 4.8 of Eco Chemie B.V. Software (Utrecht, The Netherlands). In the vicinity of the differential capacity peaks, the incremental potential steps were as small as 5 mV. Each subsequent step was applied after the electrodes were potentiostatically equilibrated during the preceeding step.

3. Results and discussion

Our preliminary studies of Li-ion intercalation into a graphite electrode showed that the behavior of this electrode, especially its long-term cyclability, improved distinctly in the presence of a small concentration of DMPC in the standard (reference) solution. A detailed report on the effect of DMPC and other organic dicarbonates on cycling and rate capabilities of graphite electrode will be reported elsewhere [5].

Fig. 1 shows slow-scan rate cyclic volumetric curves, (scan rate $v = 20$ μV/s) measured with a graphite electrode at four different temperatures: 30, 45, 60 and 80 °C. Vertical broken lines mark the boundaries of the lithiated graphite phases during Li-ion intercalation. Two-phase coexistence regions are indicated by stage numbers, for example, (1 + 2) denotes coexistence of stages 1 and 2. The so-called "solid solution" domain is designated as (4, 3), meaning that Li-ions are inserted in such a way that there is no crystallographic prove for the coexistence of phases 4 and 3. The corresponding crystallographic (0 0 2) or (0 0 4) peaks shift smoothly with potential in this domain without substantial change in its height [6–9]. 2L in this figure denotes the so-called liquid phase 2, which is characterized by a lack of Li in-plane ordering [10,11].

Note that the cell construction used in our work allowed us to obtain accurate data, thus the CV curves measured in the range of temperatures from 30 to 80 °C were strictly

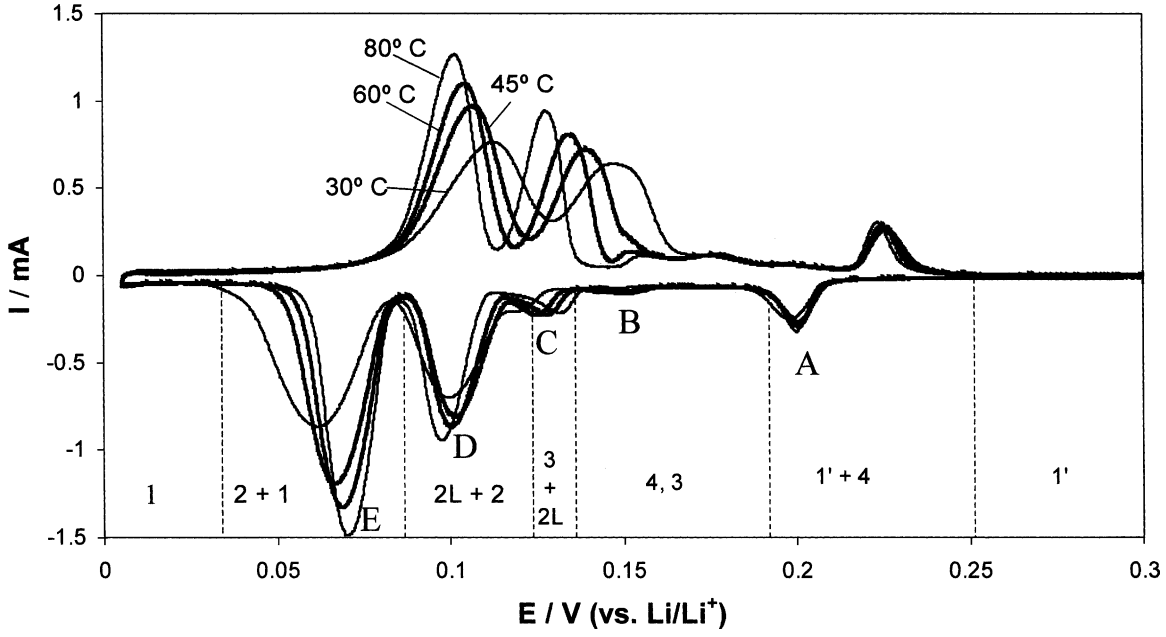

Fig. 1. A family of cyclic voltammograms measured with a graphite electrode between 0.3 and 0.005 V (vs. Li/Li^+) at four different temperatures as indicated. The scan rate was 20 μV/s. The borders between phase boundaries related to Li-intercalation during discharge are marked. Peaks from A to E designate two-phase coexistence, except for peak B, which relates to the so-called solid solution domain of the stages 4 and 3.

reproducible. Due to this fact, we were able to perform rigorous electrochemical kinetic analysis of Li-insertion and deinsertion into/from the electrode as a function of temperature. The states of the intercalation approaching thermodynamic equilibrium were also considered and compared with the well-known staging phase diagram of Li_xC_6 in the plot of the absolute temperature, T versus intercalation level, x [12,13]. Detailed kinetic analysis will be presented elsewhere [5]. Here, we shortly refer to selected, most important results.

The shape and peak-potential separation for three major cyclic volumetric peaks, A, D and E, reflect two-phase coexistence regions, as indicated in Fig. 1. Involvement of Li-ion solid-state diffusion kinetics into the intercalation mechanism results in a pronounced narrowing of the cathodic and anodic peaks A, D and E, and the decrease in their related peak-potential separations as a function of temperature.

However, the solid-state diffusion process in not the only one which determines the shape of SSCV curves shown in Fig. 1. This process is rather coupled with the accomodation of Li-ions on the guest (intercalation) sites of the host matrix. For this reason, it is of interest to check compatibility of some characteristic features of classical Li_xC_6 phase diagram [10] with the SSCV curves shown in Fig. 1. The staging phase diagram of Li_xC_6 predicts narrowing of all the two-phase coexistence domains, and a characteristic shift of the middle points of these domains towards lower values of x [10,11]. Since the middle points of the two-phase coexistence domains approximately correspond to x position of the CV peaks, it is expected that these peaks shift to lower x as the temperature increases. Comparison of this important theoretical [12,13] and experimental [10] prediction with SSCV curves in Fig. 1 requires their numerical integration and replotting in the form of I versus x. We were able to observe a small but clearly defined shift in the position of the peak E upon a temperature increase from 30 to 80°, about $\Delta x = 0.028$ (details are given in [5]). These predictions had been realized experimentally [5]. The shift in the peak position upon increasing the temperature from 30 to 80 °C, is about $\Delta x = 0.028$.

Special case presents the stability of stage 2L with temperature. It is seen in Fig. 1 that an increase in the temperature results in the shift of peaks C and D to lower and higher potentials, respectively. This may be considered as a clear manifestation of the increased stability of the stage 2L at elevated temperatures, which is in good agreement with the experimental results obtained by Dahn [6] who used a conventional slow galvanostatic charging and discharging technique.

Striking although reproducible features in Fig. 1 are that (i) the potential shift of the cathodic peak D with an increase in the temperature is considerably smaller than that for the corresponding anodic peaks, and that (ii) the saddle point between peaks E and D is much closer to zero on the current axis in the course of intercalation compared to that for deintercalation. We rationalize this fact assuming, basically, higher diffusion restrictions for the deintercalation process compared to that for the intercalation (the broader anodic peaks compared to the cathodic ones support it).

From the above consideration it is seen that SSCV, which is commonly a large-amplitude technique, is limited in its ability to distinguish between different rate-determining steps contributing to the whole intercalation–deintercalation process. In order to reach better separation between slow intercalation kinetic and thermodynamic effects (which is not straightforward in the framework of SSCV, demanding too low potential scan rates), we applied PITT [14,15]. This incremental technique may ensure a closer approach to thermodynamic equilibrium, selectively separating the various process time domains, thus providing further analysis of the Cottrell solid-state diffusion domain [4]. A principal shortcoming of this small-amplitude technique with respect to the large-amplitude SSCV technique is considerably smaller number of experimental points for the former technique (the number of practically used potential increments is always less than the number of points during a continuous linear potential sweep).

Fig. 2a and b show the plots of the differential intercalation capacity of graphite electrode, C_{int}, and the chemical diffusion coefficient of the Li-ions, D_{chem}, versus potential E, respectively (the procedure of data treatments was previously reported [3,4]). Taking into account that C_{int} can be also obtained from the slow-scan rate cyclic voltametric curve shown in Fig. 1: $C_{int}(E) = I(E)/v$, $v = 20\ \mu V/s$, both these two plots can be compared. It is seen that over the entire temperature range used, C_{int} versus E plot obtained from PITT (Fig. 2a) reveals narrower peaks than these in the same plot obtained from SSCV (Fig. 1). This means that PITT, with the appropriate potential step increments provide almost thermodynamically controlled conditions, while the high-amplitude technique, namely, SSCV, deviate to some extent from these conditions. However, the above-mentioned shortcoming of PITT complicates the measurements of the temperature dependence of C_{int} in the higher Li_xC_6 stages (compare regular shifts of peaks B and C in Fig. 1 and the obvious loss of resolution in the same potential domain on the curves in Fig. 2a).

The plots of $\log D_{chem}$ versus potential E (see Fig. 2b), show characteristic minima in the vicinity of the corresponding maxima of C_{int}. Both these extremums relate to two-phase coexistence regions, as is schematically shown in Fig. 2a and b. This behavior of an intercalation electrode is caused by the highly attractive, short-range interactions between the intercalation sites, as previously discussed [2–4]. Diffusion is an activation controlled process, thus D_{chem} is increased with temperature within the two-phase domains. The lack of resolution (due to an insufficient number of points) of $\log D_{chem}$ versus potential E curves is especially serious within the two-phase domains, thus it is difficult to obtain accurate quantitative dependence of D_{chem} as a function of potential. In addition, any reference to a

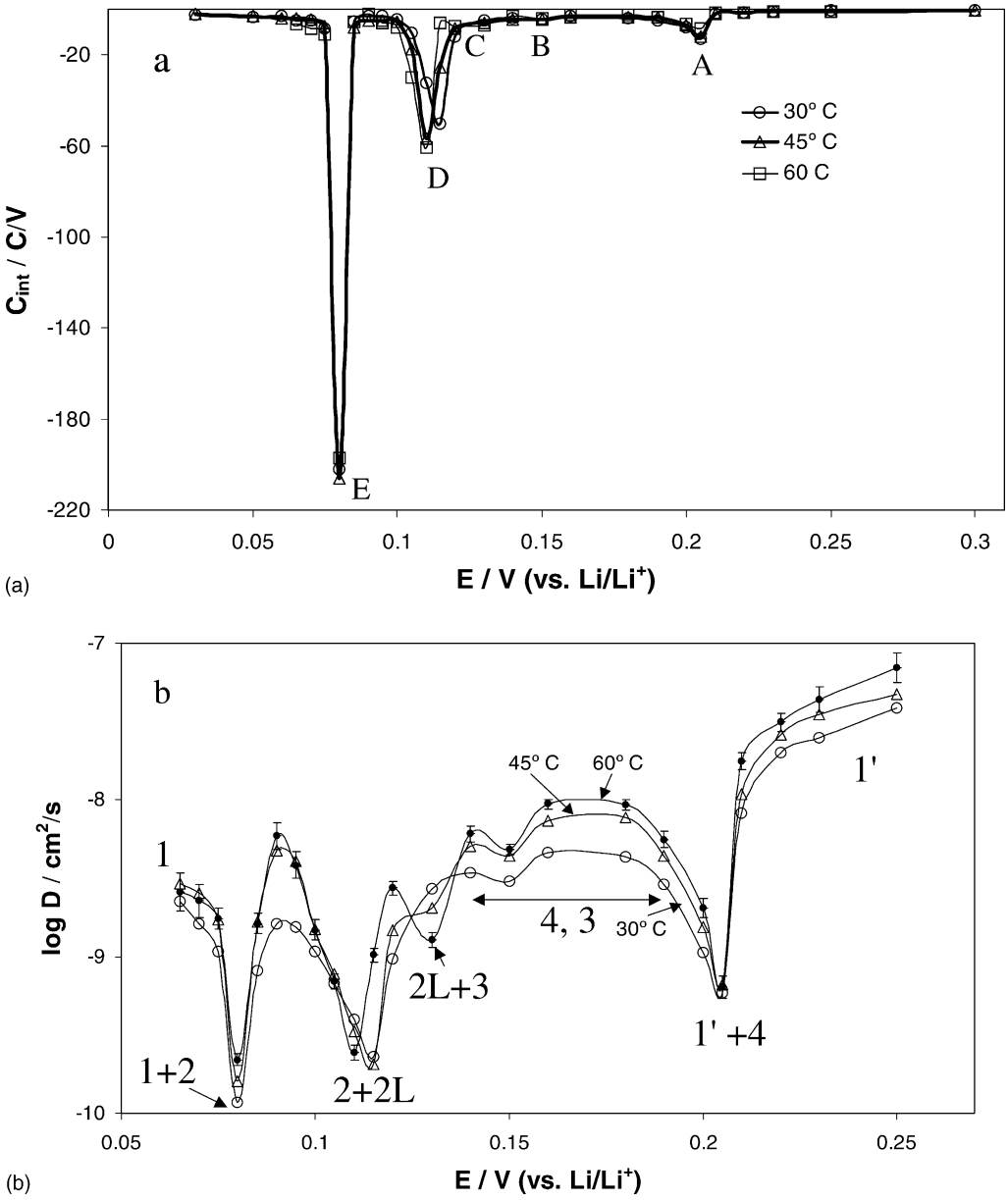

Fig. 2. Plots of potential dependencies of (a) the differential intercalation capacity, C_{int}, and (b) the chemical diffusion coefficient, D_{chem}, measured with a graphite electrode at three different temperatures: 30, 45 and 60 °C. The borders between phase boundaries are indicated.

definite chemical diffusion coefficient ascribed to a two-phase coexistence domain usually raises the question on its theoretical interpretation.

As previously reported [4], it is possible to assign to almost each potential increment a certain effective coefficient D_{chem}, once and where a Cottrell (or pseudo-Cottrell) dependence $It^{1/2}$ versus log t can be experimentally observed in the short-time domain (i.e. much below the characteristic diffusion time constant τ). Interfacial kinetics contributions, which have not been taken into account in this work, may somewhat distort the evaluated parameter $It^{1/2}$ and thus D_{chem}, as was recently pointed out by Montella [16]. Moreover, we can easily imagine a situation when on the decrease of the potential step amplitude, the whole current transient will be rather controlled by slow small droplet formation of a new phase in the bulk of the old one, as was the case of a drastic structural changes during transition from cubic to tetragonal form of spinel [17]. In this case, even pseudo-Cottrell domain cannot be followed on the experimental current transient [17]. However, the above two effects become insignificant once narrow, peak-shaped dependence of log D_{chem} versus E is discussed in a purely qualitative manner.

The contribution of the slow droplet formation to the current transients during small potential steps can be considerably minimized, and hence the number of steps (experimental points) increased within the relatively flat portion of the CV curve (and hence C_{int} versus E curve) related to the

so-called solid solution stages, namely, 4 and 3 (see Figs. 1 and 2a). Compromising between the number of points in this domain, the length of time measurements, and the subtraction of background current, one can determine accurately the values of D_{chem} as shown in Fig. 2b (errors bars are shown as an example for log D_{chem} versus potential E curve measured at 60 °C).

In a paper appeared elsewhere [18], we attempted to quantify the analysis of this interesting, in a sense, unique part of phase diagram of Li_xC_6, reinterpreting the concept of formation of a solid solution between the lithiated graphite stages 4 and 3.

4. Conclusions

Quantitative characterizations of temperature dependencies of the differential intercalation capacity and the chemical diffusion coefficient related to Li-insertion electrodes may provide challenges to both experimental studies of real physical and electrochemical processes determining batteries operation conditions and the theory of intercalation phenomena. The use of a combined application of SSCV and PITT for the characterization of intercalation electrodes in a wide range of temperatures can be useful in identifying an interplay of competing separate steps of the intercalation processes and a selection of optimum conditions for batteries operations depending on customer demands and preferences. Referring to fundamental problems of Li-ion intercalation into inorganic hosts, the above temperature dependencies may present an important bridge between the classical phase diagrams of Li_xC_6 (usually performed ex situ and in the limit of high temperatures) with in situ electroanalytical measurements at elevated temperatures. Such a comparison is useful in distinguishing between general features of the 3D intercalation mechanism and possible changes in interfacial kinetics caused by obviously complex electrochemical behavior of the solution electrolytes at elevated temperatures.

References

[1] A. Martinent, B. Le Gorrec, C. Montella, R. Yazami, J. Power Sources 97–98 (2001) 83.
[2] M.D. Levi, D. Aurbach, J. Phys. Chem. B 101 (1997) 4630.
[3] M.D. Levi, D. Aurbach, J. Phys. Chem. B 101 (1997) 4641.
[4] M.D. Levi, D. Aurbach, Electrochim. Acta 45 (1999) 167.
[5] M.D. Levi, C. Wang, D. Aurbach, in preparation.
[6] J.R. Dahn, Phys. Rev. B 44 (1991) 9170.
[7] T. Ohzuku, Y. Iwakoshi, K. Sawai, J. Elecrochem. Soc. 140 (1993) 2490.
[8] M.D. Levi, E. Levi, D. Aurbach, J. Electroanal. Chem. 421 (1997) 89.
[9] D. Aurbach, B. Markovsky, I. Weissman, E. Levi, Y. Ein-Eli, J. Electroanal. Chem. 421 (1997) 89.
[10] J.E. Fischer, C.D. Fuerst, K.C. Woo, Synth. Met. 7 (1983) 1.
[11] K.C. Woo, W.A. Kamitakahara, D.P. Di Vincenzo, D.S. Robinson, H. Mertwoy, J.M. Milliken, J.E. Fischer, Phys. Rev. B 50 (1983) 182.
[12] S.E. Millman, G. Kirczenow, Phys. Rev. B 26 (1982) 2310.
[13] J.R. Dahn, D.C. Dahn, R.R. Haering, Solid State Commun. 42 (1982) 179.
[14] W. Weppner, R.A. Huggins, J. Electrochem. Soc. 124 (1977) 1569.
[15] C.J. Wen, B.A. Boukamp, R.A. Huggins, W. Weppner, J. Electrochem. Soc. 126 (1979) 2258.
[16] C. Montella, J. Electroanal. Chem. 518 (2002) 61.
[17] M.D. Levi, K. Gamolsky, D. Aurbach, U. Heider, R. Oesten, J. Electrochem. Soc. 147 (2000) 25.
[18] M.D. Levi, C. Wang, D. Aurbach, Z. Chvoi, J. Electroanal. Chem., submitted for publication.